

Numerical and Experimental Analysis of Friction Stir Welding of Aluminum Alloy AA2024-T4



Deepak Kumar, Md. Parwez Alam, and A. N. Sinha

Abstract The paper deals with the influence of heat input on metallurgical and mechanical properties that have been investigated through experimental and numerical investigations. Two process parameters were taken to conduct the experiments. Thermocouples were used to measure temperature distributions. The heat generated during the friction stir welding (FSW) affected the grain refinements strongly, which were revealed with optical microscope (OM) micrographs. A three-dimensional model was developed to obtain the simulated temperature during the FSW of AA 2024-T4. The simulated temperature data was very close to that of the experimental data. It was observed that the heat generation depends on both transverse and rotational speed, and the peak temperature obtained was about 80% of the melting point of base metal. Additionally, tensile tests were performed for joint strength.

Keywords Friction stir welding · Optical microscope · AA 2024-T4 · Tensile test

1 Introduction

Friction stir welding (FSW) is a solid-state thermomechanical joining technique. It is an environmental-friendly, energy-efficient, and ideal welding technique that produces high-performing joints at a low cost. A rotating cylindrical tool having two parts, shoulder and pin, is used. The pin is fed in the joint line of two clamped sheets until the shoulder touches its surface and subsequently traversed along the joint line [1]. Frictional and plastic deformational heat is generated during the process, which softens the material. During the forwarding movement of the tool along the weld line, it extruded behind the pin, and high pressure assists in forged consolidation of the weld [2]. A schematic diagram illustrates the FSW process, shown in Fig. 1. In the FSW process, heat generation has crucial effects on the weld joints' mechanical properties and metallurgical characteristics. A full understanding of heat generation is essential for controlling the joints' mechanical properties and metallurgical

D. Kumar · Md. P. Alam (✉) · A. N. Sinha
Mechanical Engineering Department, NIT Patna, Ashok Rajpath Patna 800005, India
e-mail: parwez.me13@nitp.ac.in

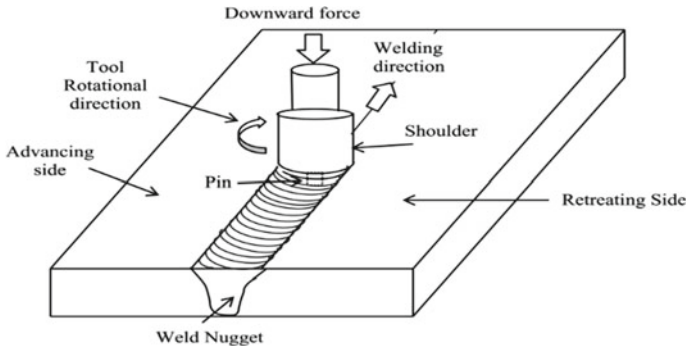


Fig. 1 Schematic representation of the FSW process [3]

characteristics. Numerical modeling offers an excellent prospect for understanding different phenomena of the FSW. For FSW, several heat generation models have been developed which describe friction and plastic deformation as the primary heat source.

Abdul-Sattar et al. [4] analyzed the temperature distribution through experimental work and modeling and observed higher temperature at the advancing side. Cartgueen et al. [5] concluded that the rate of heating and peak temperature highly depends on the transverse and rotational speed of the tool, respectively. Gadakh et al. [6] constructed a model for comparing heat generation by FSW using a taper and straight cylindrical pin and observed that the taper pin generated less heat than the straight pin. Zhang et al. [7] found that the contact area between shoulder-workpiece contributes more in heat generation than pin-workpiece. Bastier et al. [8] developed a heat transfer model for the FSW process. They observed that the plastic and frictional heat generation was equal to 4.4% and 95.6% of the total heat generation, respectively. Rajamanickam et al. [9] developed a transient model in which heat input from the tool shoulder alone was considered. The maximum temperature gradients were observed to be located just beyond the shoulder edge in both longitudinal and lateral directions. Many studies show that the moving heat technique is a reliable method to simulate heat generation during the FSW process. The use of ANSYS software can obtain the FSW process's temperature outputs at each required time step. In this study, two different process parameters had been used to perceive its sound effect on FSW temperature distribution. With the help of ANSYS software, a thermal model was developed to simulate the thermal history of AA2024-T4 during FSW. The model was validated by experimental data. Tensile tests were carried out to find out the joint strength. Besides, the microstructure of friction stir welded AA2024-T4 was also evaluated.

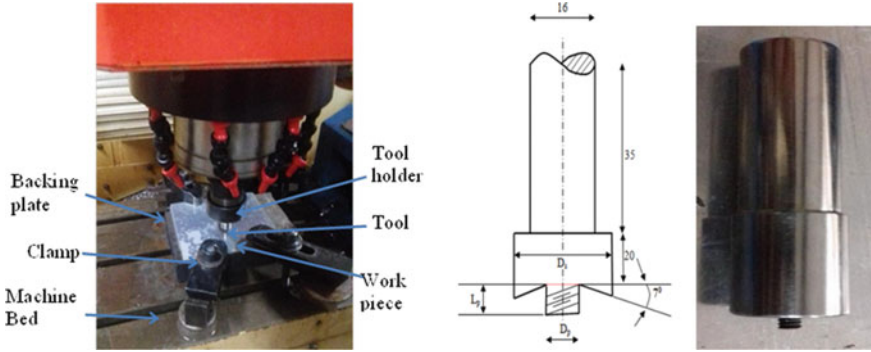


Fig. 2 Experimental setup and FSW tool with its geometry

2 Experimental Investigation

AA2024-T4 sheets ($120 \times 80 \times 3$ mm) were used in the present study. A vertical milling machine was used for the joining of these sheets. Figure 2 shows the experimental setup and FSW tool with its geometry. The tool was made of AISI H13 tool steel material. Tool shoulder was curved, and its diameter (D_s) was 18 mm. The pin was straight cylindrical threaded, and its diameter (D_p) and length (L_p) were 4.5 mm and 2.7 mm, respectively. The input parameters, 700, 850, and 1000 rpm as rotational speed, and 20, 30, and 40 mm/min as transverse speed, were taken for machine process parameters. 0.1 mm plunge depth was given in all experiments.

For temperature measurement, thermocouples were inserted in two holes, which were drilled at 15 mm and 25 mm away from the joint line. ASTM standards were followed for tensile samples. For metallurgical characterization, metallographic images were captured by an optical microscope (OM) after polishing and etching the samples.

3 Numerical Investigation

3.1 Heat Transfer Model

Developing a thermal profile model for the FSW process is an ideal beginning for simulating the process using simulation software. The model helps calculate the approximate heat generation value by the FSW process, which can be used as the input for evaluating the temperature distribution using ANSYS 17.2. Understanding the FSW process is essential to develop a sound mathematical model. Many researchers over the years have tried to develop mathematical models to predict heat generation. Hamilton et al. [10] developed the most suitable model for calculating the heat flux.

As per the model, the generation of heat is constant during the intermediate period of welding. During the beginning and end, the process is highly dynamic. When the welding is started, the heat increases exponentially, and at the end, it decreases in the same manner. In the heat transfer analysis, the transient temperature (T), the function of time (t), and spatial coordinates (x, y, z) are obtained by Eq. (1).

$$k \left(\frac{\partial^2 T}{\partial x^2} + \frac{\partial^2 T}{\partial y^2} + \frac{\partial^2 T}{\partial z^2} \right) + Q_{\text{int}} = c\rho \frac{\partial T}{\partial t} \quad (1)$$

where T , k , Q_{int} , C , and ρ are the temperature (K), thermal conductivity (W/m.K), internal heat source rate, specific heat (J/kg.K), and material density, respectively. Heat loss from the workpiece surfaces to the ambient due to convection and radiation heat transfer, but heat loss from the workpiece's bottom surface is due to conduction. But the evaluation of this heat loss is not a simple task; this can be evaluated by the simple convection Eq. (2).

$$q_b = \beta_b (T - T_0) \quad (2)$$

where β_b is the convection coefficient of heat transfer, in W/(m².K), between the backing plate and the workpiece. 200 W/m² K used for β_b value. In FSW, heat is generated by friction as well as plastic deformation. But in this present work, plastic deformational heat is not considered. Hence, only frictional heat is used as the heat source in this numerical investigation. It is assumed that the heat flux (rate of heat generation) is uniformly distributed at the pin tool shoulder Chao et al. [11]. The equation is used to obtain a heat generation (q_r) rate.

$$q_r = \frac{3Qr}{2\pi(r_o^3 - r_i^3)} \quad (3)$$

$$Q = \frac{\omega\pi\mu F(r_o^2 + r_o r_i + r_i^2)}{45(r_o + r_i)} \quad (4)$$

where F is a downward force (15 KN), ω is the tool rotational speed, μ is the coefficient of friction (0.3), Q is the total heat input, r_o and r_i are the shoulder radius and pin radius, respectively.

3.2 Finite Element Model

In this study, ANSYS 17.2 was used to carry out the transient heat transfer analysis. By using the ANSYS software, the workpiece of size 125 × 80 × 3 mm had been modeled. Table 1 gives the temperature-dependent properties of AA 2024-T4. Two different meshes were required for conducting the simulation. One of the elements selected was SOLID 70, a solid 3D element to predict the nodal solutions. Another

Table 1 Temperature-dependent properties of AA2024-T4 [12]

Temperature (K)	290	373	473	573	673
Specific heat capacity (Jkg ⁻¹ K ⁻¹)	864	921	1047	1130	1172
Thermal conductivity (Wm ⁻¹ K ⁻¹)	120	134.4	151.2	172.2	176.4
Yield strength (MPa)	350	331	140	45	21

one was SURF 55, a surface element used for allocating convection properties to the model. 293 K temperature was taken for initial as well as ambient temperature. 30 W/(m².K) was taken for convective coefficient at the top surfaces of the plates for natural convection between air and aluminum alloy surfaces.

4 Results and Discussion

4.1 Temperature Distribution

Figure 3a–c shows the temperature distribution of temperature contour at 30, 150, and 270 s when the pin is translated along the joint line. The transient temperature is affected by both rotational speed and transverse speed. Also, it is affected by conduction convection and radiation. The peak temperature of friction stir welding of aluminum alloy 2024-T4 using the thermal model at different input process parameters is shown in Fig. 3d–h. Figure 3d–f shows that at constant welding speed (20 mm/min), the peak temperature increases when increasing the rotating speed. When the rotating speed increases, it increases the strain rate and plastic dissipation in the stir zone, which increases the peak temperature. Increased rotating speed from 700 to 1000 rpm leads to significant changes in the peak temperature. At 1000 rpm–20 mm/min, peak temperature 732.67 K is observed. Similar trends were observed by Cartigueyen et al. [5]

Figure 3e–h shows the effect of transverse speed on the peak temperature at 850 rpm. As the transverse speed increases from 20 mm/min to 40 mm/min, it decreases the peak temperature from 712.67 K to 652.128 K in the stir zone at a given point. With an increase in transverse speed, the time for which the tool is in contact with the workpiece decreases; hence, frictional heat decreases, which leads to the temperature drop at the welding position. At transverse speed 40 mm/min and constant rotational speed 850 rpm, peak temperature 652.128 K is observed, as shown in Fig. 3h.

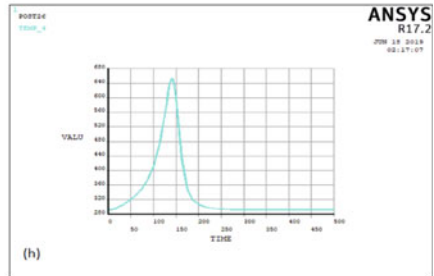
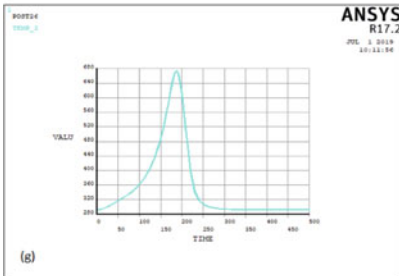
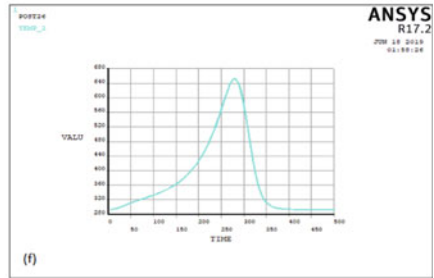
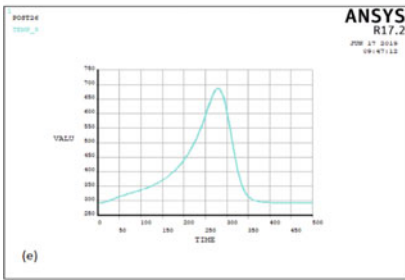
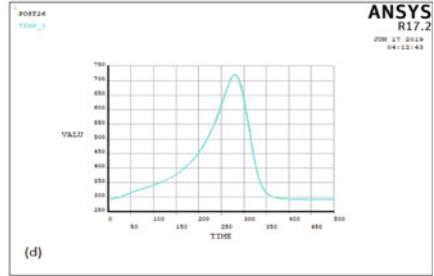
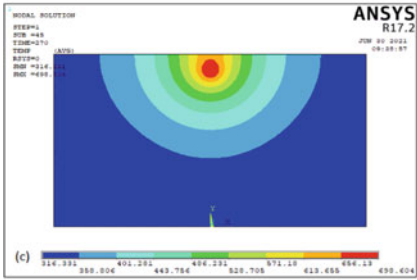
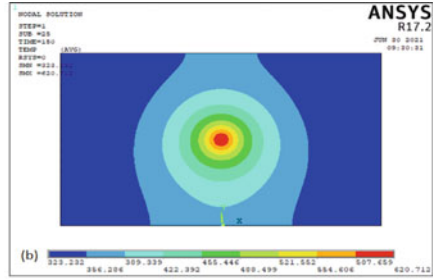
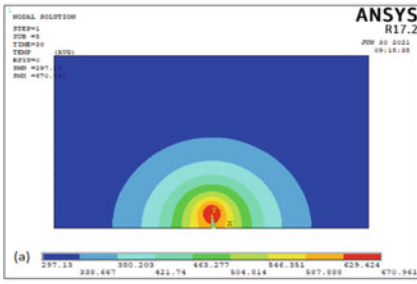


Fig. 3 Simulated temperature distribution of temperature contour at **a** 30 s, **b** 150 s, **c** 270 s and process parameters, **d** 1000 rpm and 20 mm/min, **e** 850 rpm and 20 mm/min, **f** 700 rpm and 20 mm/min, **g** 850 rpm and 30 mm/min, **h** 850 rpm and 40 mm/min

Table 2 Comparison between experimental temperature and simulated temperature

Sample no.	Parameters		Experimental temp. (K)		Simulated temp. (K)		% Error	
	Rotational speed (rpm)	Transverse speed	Temp. at P1 (max)	Temp. at P2 (max)	Temp. at P1 (max)	Temp. at P2 (max)	P1	P2
1	700	20	446	371	428	361	4	2.7
2	850	20	456	377	441	368	3.3	2.4
3	1000	20	465	385	449	372	3.4	3.4
4	700	30	424	356	408	350	3.8	1.7
5	850	30	436	361	424	358	2.8	0.83
6	1000	30	453	379	438	366	3.3	3.4
7	700	40	411	353	395	344	3.8	2.5
8	850	40	430	361	415	353	3.5	2.2
9	1000	40	443	369	427	360	3.6	2.4

4.2 Validation of the Thermal Model

Table 2 gives the comparison between experimental temperatures obtained using the thermocouples placed at a distance (P1) 15 mm and (P2) 25 mm away from the welding line and simulated temperature. The table gives that the experimentally measured temperature and the simulated temperature values lie close to each other, and the % error varies from 2.8% to 4% at location P1 and 0.83% to 3.4% at location P2. The variation between these two temperatures is due to ignoring the plastic deformational heat and heat generated by the pin of the tool.

4.3 Tensile Test Study

The tensile tests were carried out by an electromechanical universal testing machine. 1 mm/min feed rate was used for the testing. Nine welded samples and a base material sample were tested. For each condition, three specimens were tested. After performing the experimentation and testing, it was observed that the samples had failed due to localized softening at the stir zone / HAZ boundary.

Figure 4a shows the standard force (MPa) vs. strain relation of the tensile specimens, which were prepared from the plate’s joint by friction stir welding at constant welding speed but varying rotational speed. 247 MPa ultimate tensile is observed at 700 rpm, but at 1000 rpm, it is increased to 343 MPa, which is approximately 80% of the base material’s ultimate tensile strength. In this study, it is observed that for a given set of rotational parameters, the joint strength increased as the rotational speed had increased when welding speed was kept constant. Figure 4b shows the joint’s strength for different welding speeds when the rotational speed is kept constant.

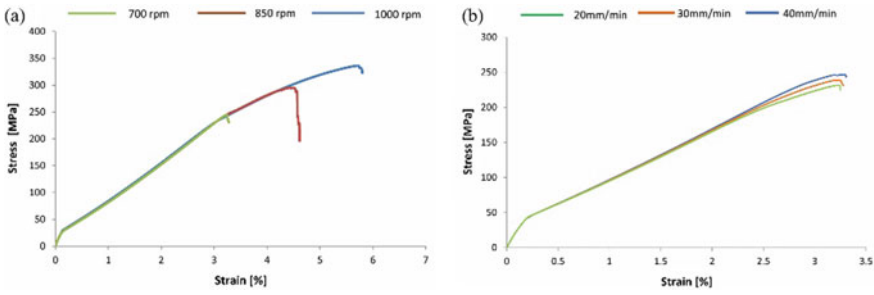


Fig. 4 Stress-strain diagram at **a** constant transverse speed, **b** constant rotational speed

It is observed that the strength of the joint increased when the welding speed had increased for the given set of welding speed parameters.

4.4 Microstructural Analysis

As the weld zone is affected by the thermal cycle during the process, it leads to a significant microstructure change. Three different zones were observed, namely stir zone (SZ), thermomechanical affected zone (TMAZ), and heat-affected zone (HAZ), as shown in Fig. 5. In the stir zone (SZ), there is direct contact between the pin and the material, due to which the material experiences deformation, heating, and friction. The thermomechanical affected zone (TMAZ) and heat-affected zone (HAZ) are not in contact with the tool. TMAZ is subjected to high temperature and deformation, and the heat emitted from the contact zone between the material and the tool affects the HAZ. It is clear from Fig. 5 that the SZ has the finest grain size as it undergoes severe plastic deformation; hence, the weldment's strength could be enhanced.

Fig. 5 Optical micrograph of friction stir welding region

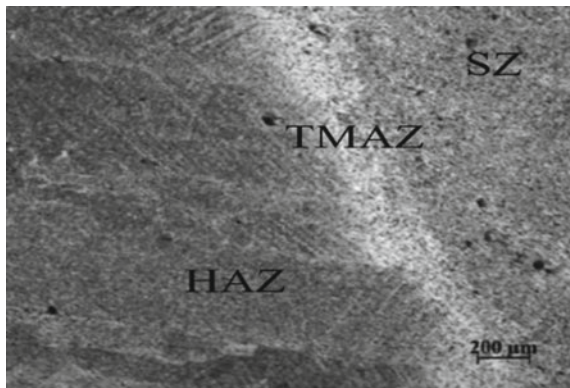


Figure 6 shows the microstructure of base material and stir zone at different rotation and welding speeds. It was observed that the decrease of grain size from base material at constant welding speed 20 mm/min but decreasing rotational speed from 700 to 1000 rpm. It was also found that the constant rotational speed, 700 rpm, as the welding speed increases, the grain size is decreasing from the parent material grain size.

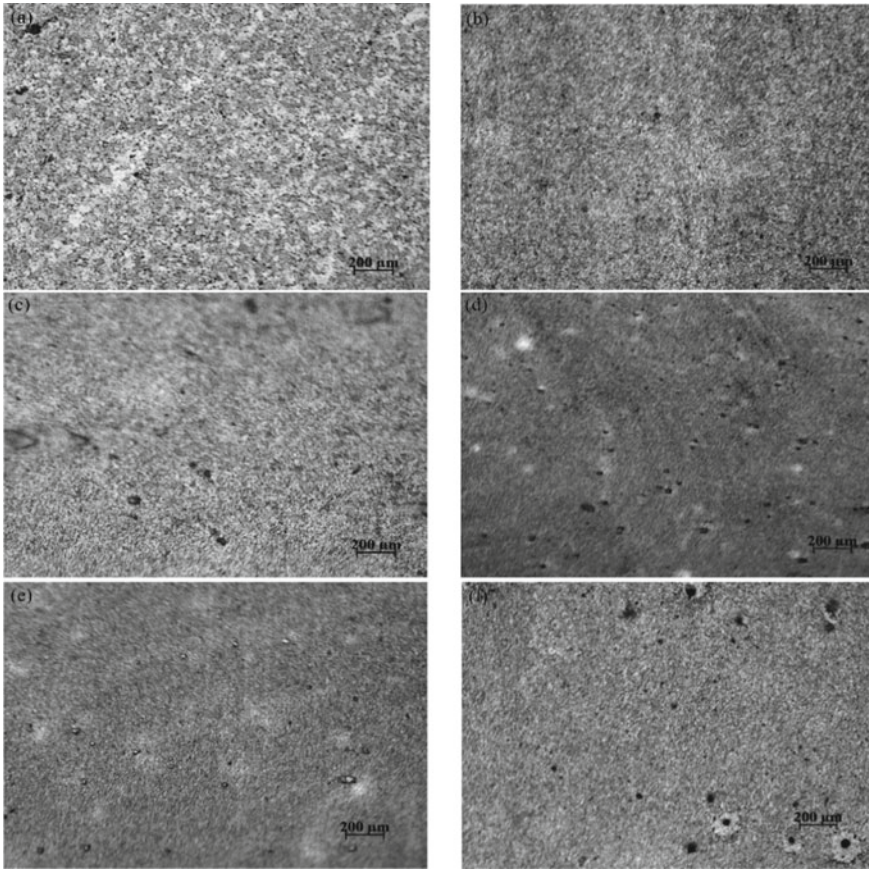


Fig. 6 Optical microstructure of **a** base material and stir zone of processed AA 2024-T4, **b** 1000 rpm-20 mm/min, **c** 850 rpm-20 mm/min, **d** 700 rpm-20 mm/min, **e** 700 rpm-30 mm/min, **f** 700 rpm-40 mm/min

5 Conclusions

Experimental and numerical investigations of FSW have provided many conclusions and silent features, which are summarized as follows:

- It is found that the tensile strength increases as both rotational and transverse speeds increase for a considered range of parameters.
- A good agreement between numerically and experimentally measured temperatures has been obtained at different locations. The maximum difference in temperature is observed to be 4% near the weld zone.
- The results show that the peak temperature increases as the rotational speed increases and decreases as the welding/ tool transverse speed increases.
- The increase in temperature affects the grain size, which further affects the joint properties.

References

1. Mishra RS, Ma ZY (2005) Friction stir welding and processing. *Mater Sci Eng R Rep* 50(1–2):1–78.41
2. Bozzi S, Etter AL, Baudin T, Robineau A, Goussain JC (2008) Mechanical behaviour and microstructure of aluminum-steel sheets joined by FSSW. *Texture Stress Microstruct*
3. Alam MP, Sinha AN (2019) Fabrication of third generation Al–Li alloy by friction stir welding: a review. *Sādhanā* 44(6):1–3
4. Abdul-Sattar M, Tolephih MH, Jweeg MJ (2012) Theoretical and experimental investigation of transient temperature distribution in friction stir welding of AA 7020–T53. *J Eng* 18(6):693–709
5. Cartigeyen S, Suresh OP, Mahadevan K (2014) Numerical and experimental investigations of heat generation during friction stir processing of copper. *Proc Eng* 1(97):1069–1078
6. Gadakh VS, Adepu K (2013) Heat generation model for taper cylindrical pin profile in FSW. *J Market Res* 2(4):370–375
7. Zhang Z, Qi WU, Zhang HW (2014) Numerical studies of effect of tool sizes and pin shapes on friction stir welding of AA2024–T3 alloy. *Trans Nonferrous Metals Soc China* 24(10):3293–301
8. Bastier A, Maitournam MH, Van Dang K, Roger F (2006) Steady state thermomechanical modelling of friction stir welding. *Sci Technol Weld Joining* 11(3):278–288
9. Rajamanickam N, Balusamy V, Thyla PR, Hari Vignesh G (2009) Numerical simulation of thermal history and residual stresses in friction stir welding of Al 2014–T6. *J Sci Ind Res* 68:192–198
10. Hamilton C, Dymek S, Sommers A (2008) A thermal model of friction stir welding in aluminum alloys. *Int J Mach Tools Manuf* 48(10):1120–1130
11. Chao YJ, Qi X, Tang W (2003) Heat transfer in friction stir welding—experimental and numerical studies. *J Manuf Sci Eng* 125(1):138–145
12. Shi L, Wu CS (2017) Transient model of heat transfer and material flow at different stages of friction stir welding process. *J Manuf Process* 25:323–39